











## LETTER

**Particulate organic carbon sedimentation triggers lagged methane emissions in a eutrophic reservoir**

Andrés Martínez-García <sup>1,2</sup> Ignacio Peralta-Maraver <sup>1,2\*</sup> Eva Rodríguez-Velasco <sup>1,2</sup> Gema L. Batanero <sup>1</sup>  
Miriam García-Alguacil <sup>1,2</sup> Félix Picazo <sup>1,2</sup> Juan Calvo <sup>2,3</sup> Rafael Morales-Baquero <sup>1</sup> Francisco J. Rueda <sup>2,4</sup>  
Isabel Reche <sup>1,2\*</sup>

<sup>1</sup>Departamento de Ecología and Instituto del Agua, Universidad de Granada, Granada, Spain; <sup>2</sup>Research Unit Modeling Nature (MNat), Universidad de Granada, Granada, Spain; <sup>3</sup>Departamento de Matemática Aplicada, Universidad de Granada, Granada, Spain; <sup>4</sup>Departamento de Ingeniería Civil, Universidad de Granada, Granada, Spain

**Scientific Significance Statement**

Reservoirs possess a dual and substantial role in the global carbon cycle, acting as carbon sink or source depending on the budget between sedimentation of particulate organic carbon (POC) and CO<sub>2</sub> and CH<sub>4</sub> emissions. However, these processes can operate at different time scales. Despite their importance, a great knowledge gap exists in understanding the phenology of POC sedimentation, particularly the role of acidic polysaccharides (APs) of phytoplanktonic origin in promoting aggregation into particulates that influence carbon export to sediments. Our study indicates a synchrony between POC and APs sedimentation rates and a significant 2-week lag with the methane emissions following POC sedimentation. This delay emphasizes the importance of time-integrated studies for a comprehensive understanding of carbon budgets within reservoirs.

**Abstract**

Reservoirs act as carbon sinks when sedimentation of particulate organic carbon (POC) exceeds CO<sub>2</sub> and CH<sub>4</sub> emissions. Here, we study the poorly explored process where phytoplankton-derived acidic polysaccharides (APs) aggregate into particulate organic matter, promoting carbon export to sediments. This source of POC in sediments can mineralize to CO<sub>2</sub> and CH<sub>4</sub> over various timescales. Our research, centered on a Mediterranean reservoir, elucidates phenological trends of APs and POC sedimentation and identifies their predominant drivers. Our findings present synchronic sedimentation patterns of POC and APs but identify a 2-week delay

\*Correspondence: [peraltamaraver@ugr.es](mailto:peraltamaraver@ugr.es); [ireche@ugr.es](mailto:ireche@ugr.es)

**Associate editor:** Monika Winder

**Author Contribution Statement:** IR, RM-B, FJR, and JC conceived the study and obtained the funds. AM-G led the fieldwork and the collection of biogeochemical data with the help of IP-M, ER-V, GLB, FP, MG-A, RM-B, FJR, and IR. AM-G performed the laboratory analysis with help of GLB and MG-A. AM-G and IP-M performed the data analysis and graphical representation of the results. AM-G, IR, and IP-M wrote the first draft of the manuscript, and all authors contribute to the preparation of the final draft.

**Data Availability Statement:** Additional Supporting Information can be found in the online version of this article, including an extended version of methods and supplementary figures and tables. The dataset associated with this paper is available from DRYAD (<https://doi.org/10.5061/dryad.73n5tb33m>).

Additional Supporting Information may be found in the online version of this article.

This is an open access article under the terms of the [Creative Commons Attribution](https://creativecommons.org/licenses/by/4.0/) License, which permits use, distribution and reproduction in any medium, provided the original work is properly cited.

between POC sedimentation and CH<sub>4</sub> emissions. Despite its eutrophic status, our data demonstrate this reservoir's role as a carbon sink, sequestering 4.33 g C m<sup>-2</sup> yr<sup>-1</sup>. This highlights the need to consider various time scales when quantifying carbon budgets in reservoirs.

Today it is well established that inland waters play a relevant and dual role in the global carbon cycle (Tranvik et al. 2009, 2018; Battin et al. 2009). While reservoirs emit substantial amounts of greenhouse gases, such as CO<sub>2</sub> and CH<sub>4</sub> (Raymond et al. 2013; Deemer et al. 2016), they also play a role in sequestering carbon in their sediments (Anderson et al. 2014, 2020; Mendonça et al. 2017). Indeed, the global estimations of carbon sequestration in inland water sediments are similar to that observed on the ocean floor (Tranvik et al. 2009; Cartapanis et al. 2018). These global estimates range between 0.06 and 0.25 Pg C yr<sup>-1</sup> (Mendonça et al. 2017; Anderson et al. 2020), and reservoirs have a disproportionately high capacity for carbon storage relative to their area (Cole et al. 2007; Teodoru et al. 2013; Mendonça et al. 2017). While CO<sub>2</sub> and CH<sub>4</sub> fluxes at the water-atmosphere interface occur on a contemporary scale, carbon sequestered in sediments becomes integrated into an extended cycle with medium- and long-term transformations (Sobek et al. 2009; Mendonça et al. 2017). Consequently, inland water systems could act as important carbon storage sites, despite their relatively elevated greenhouse gas emissions depending on the budget between carbon emissions and sequestration in the sediments in a definite time interval (Quadra et al. 2020). Although great progress has been made in recent years in measuring the carbon emissions in inland waters across different scales and biomes (e.g., Raymond et al. 2013; Deemer et al. 2016; León-Palmero et al. 2020a), our knowledge of the temporal patterns of carbon export and burial efficiency in sediments is still very limited (de Vicente et al. 2009; Teodoru et al. 2013; Isidorova et al. 2019a). Recently, Grasset et al. (2021) have experimentally demonstrated that the quantity and quality of the particulate organic matter exported towards the sediments can be fundamental in methane production. In fact, they found increases up to 34% in CH<sub>4</sub> production associated with autochthonous inputs of phytoplanktonic particulate organic matter. Therefore, the carbon budget across various timescales should be considered instrumental in assessing the carbon sequestration capabilities of lakes and reservoirs and, consequently, their relevance as components in mitigating climate change.

Sedimentation of both allochthonous and autochthonous particulate organic carbon (POC) is the primary pathway of carbon export to the sediments in reservoirs (von Wachenfeldt et al. 2008; de Vicente et al. 2009; Teodoru et al. 2013; Morales-Pineda et al. 2016; Quadra et al. 2020). A fraction of POC flocculates, sediments, and is subsequently buried in the anoxic sediments during the stratification (von Wachenfeldt et al. 2008; von Wachenfeldt and Tranvik 2008; Sobek et al. 2009).

A fraction of POC undergoes mineralization, leading to the release of CO<sub>2</sub> or CH<sub>4</sub> in terms of days, weeks, or years (Huang et al. 2019; Isidorova et al. 2019b; Quadra et al. 2020). This coagulation, flocculation, and sedimentation of POC can be mediated by transparent exopolymer particles (TEPs) and their acidic polysaccharides (APs) precursors (Engel et al. 2004; de Vicente et al. 2009; Danger et al. 2012). TEPs and APs constitute a relevant fraction of the total organic carbon in aquatic environments, occurring in particulate and dissolved forms (Passow 2002a; Thornton et al. 2007). They have mostly an autochthonous origin, produced by exudates from phytoplankton and cyanobacteria, and heterotrophic prokaryotes (Passow 2002a,b; Ortega-Retuerta et al. 2010; Iuculano et al. 2017), although Attermeyer et al. (2019) have also reported a terrestrial origin of TEPs in boreal aquatic ecosystems. Therefore, biological productivity (chlorophyll *a* [Chl *a*] as a surrogate) is usually the primary driver of TEPs and APs concentration (Liu et al. 2015; Callieri et al. 2017). APs are adhesive substances (Engel 2000) that function as binding agents resulting in coagulates that are ballasted by organic or mineral components such as dust and cations, inducing aggregation (Engel et al. 2004). Considering all the above, the phenology of POC sedimentation rates may be influenced by the APs fraction derived from primary productivity. Nevertheless, a lack of temporal resolution studies of the role of these compounds in the POC sedimentation in lakes and reservoirs has precluded a thorough examination of this relationship and its potential implication in carbon emissions from sediments.

Even though reservoirs are the prevalent aquatic ecosystem in the Mediterranean biome (Lehner and Döll 2004), our understanding of their carbon budget is less known, and they usually are underrepresented in the global carbon flux estimations (e.g., Barros et al. 2011; Deemer et al. 2016; Golub et al. 2023). For instance, a recent leading review on carbon burial in the sediments of 344 lakes and 59 reservoirs worldwide only included 2 reservoirs located in the Mediterranean basin (Mendonça et al. 2017). Mediterranean reservoirs exhibit a unique phenology marked by extreme fluctuations in hydrological and thermal conditions. They usually are monomictic, with only one stratification period, leading to hypolimnetic isolation and anoxia. It is expected that global change increases stratification duration and hypolimnion deoxygenation (Jane et al. 2021; Woolway et al. 2021, 2022) and eutrophication (Beaulieu et al. 2019), enhancing autochthonous organic matter production and carbon export towards sediments (Anderson et al. 2014, 2020), increasing likely methane production (Jansen et al. 2022).

Here, we explore the phenology of POC sedimentation in a eutrophic Mediterranean reservoir during the stratification and mixing periods. We quantify the sedimentation rates of APs and POC and examine the role of different drivers. In addition, we contextualize our findings alongside measurements of CO<sub>2</sub> and CH<sub>4</sub> emissions conducted simultaneously in the study reservoir (Rodríguez-Velasco et al. unpublished data) to determine the annual carbon budget. To the best of our knowledge, this is the first study to capture both carbon emission and sedimentation fluxes at the same temporal scale across the system's phenology. It underscores the relevant role of temporal integration in carbon budgets in reservoirs, even if not scaled globally. Our research holds substantial implications for forecasting future carbon sedimentation in Mediterranean reservoirs, particularly considering the expected intensification of eutrophication and more extended stratification periods due to global change.

### Material and methods

We conducted the study at the Cubillas reservoir (37°16'34"N, 3°40'24"W), located in Granada, Spain (Fig. 1). See Supporting Information Table S1 for further characterization of the study site. A previous study including Cubillas reported Chl *a* concentration values between 8.4 and 17.8 μg L<sup>-1</sup> (León-Palmero et al. 2020b), so it can be considered as a eutrophic reservoir according to the trophic state index proposed by Carlson (1977). We carried out weekly samplings for 2 yr (June 2020–2022). We installed eight sedimentation traps (Hydro-Bios Saarsø 444,000), four at 2 m (S1–S4 in Fig. 1), and four at ca. 7 m depth (D1–D4 in Fig. 1).

The use of sediment traps is a widespread technique to determine particulate organic matter (POM) sedimentation (e.g., de Vicente et al. 2009; Teodoru et al. 2013); however, it can present certain limitations that require attention, particularly in turbulent waters or in locations affected by sediment resuspensions (Kozerski 1994). Along with sampling through sediment traps, we collected water samples using a UWITEC sampling bottle of 5 liters to determine Chl *a*, divalent cations, and cyanobacteria abundance. We put the samples for cyanobacteria in cryovials, fixed with 1% paraformaldehyde and 0.05% glutaraldehyde, and subsequently frozen and stored them at -80°C until further analysis. We also measured temperature and conductivity in the water column using a multiparametric probe (Conductivity, temperature, and depth, CTD).

To determine the APs concentration and its sedimentation rates, we modified the Thornton et al. (2007) protocol (more details in Supporting Information and Fig. S1). To determine the Ca and Mg concentrations, we filtered the samples using a 0.22-μm pore size PTFE (polytetrafluoroethylene) syringe filter. Then, we quantified these cations by ionic chromatography. We determined the abundance of cyanobacteria using a FACScalibur flow cytometer following the protocols described by Gasol and del Giorgio (2000). We determined Chl *a* concentration following the spectrophotometric protocol described in APHA (1992). Note that we consider Chl *a* concentration as a surrogate of all phytoplanktonic groups presented in the reservoir, including cyanobacteria.

To obtain POM, we filtered a varying volume of the sedimentation trap collectors using combusted GF/F glass-fiber filters. The filters were dried at 60°C for 12 h and weighed to

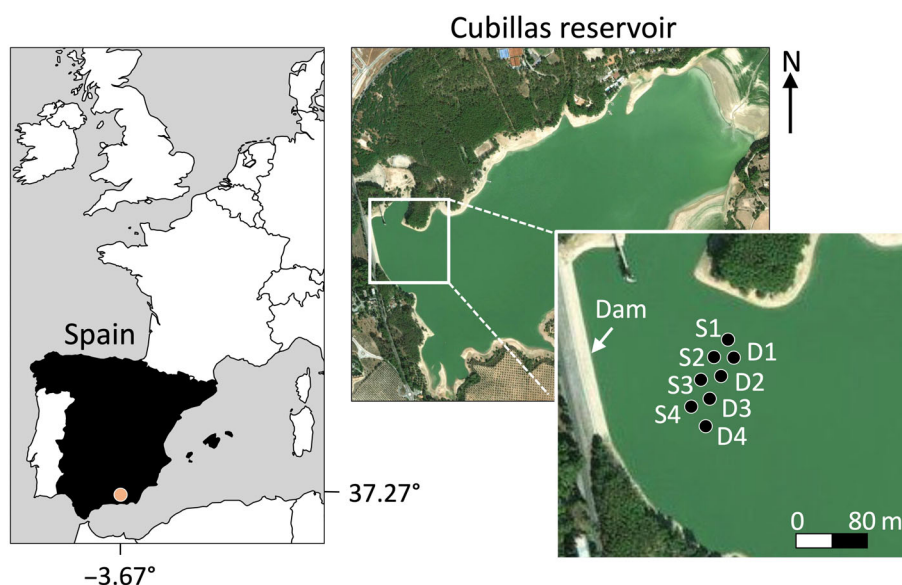


**Fig. 1.** Geographical location of the study reservoir. The zoomed picture of the Cubillas reservoir includes the deployment site of the sediment traps. S1–S4 represent the surface (2 m) traps and D1–D4 represent the deep (ca. 7 m) traps.

determine the dry weights (organic and inorganic material). Then, we used the loss on ignition method (Heiri et al. 2001) to calculate POM concentration. We combusted the GF/F filters at 550°C for 4 h and weighed them again to obtain the particulate inorganic material. We calculated POM as the difference between the filter weights before (total dry weight) and after (inorganic material) combustion. We calculated POM sedimentation rates ( $S_{\text{POM}}$ ) as in de Vicente et al. (2009):

$$S_{\text{POM}} = M \times V_{\text{T}} \times V_{\text{F}}^{-1} \times A^{-1} \times T^{-1}$$

where  $M$  represents the POM mass of a specified volume ( $V_{\text{F}}$ ) of the homogenized settling suspension. The volume of the trap collector ( $V_{\text{T}}$ ) was 0.25 liters, the collection area ( $A$ ) was 149.57 cm<sup>2</sup>, and  $T$  is the time interval between consecutive sampling events when settling matter was collected. We converted POM into POC using an elemental analyzer (Thermo Scientific model Flash 2000). Then, to identify the primary predictors of sedimentation rates of APs and

POC, we employed a multiple linear regression approach (more details in Supporting Information; extended methods). Statistical analyses and visualizations were carried out using R software version 4.0.5 (R Core Team 2023).

Finally, we compare the carbon exported to sediments in the study reservoir with the CO<sub>2</sub>, CH<sub>4</sub>, and total (CO<sub>2</sub> + CH<sub>4</sub>) emissions measured simultaneously by Rodríguez-Velasco et al. (unpublished data). Briefly, we measured CO<sub>2</sub> and CH<sub>4</sub> emissions using a PICARRO G2508 Cavity Ring-Down Spectrometer connected to a floating chamber on the reservoir surface, recording from four to six measurements daily. Flux calculations were based on Eq. 1 (Zhao et al. 2013):

$$\text{Flux}_{\text{water-air}} = \frac{86,400 \cdot M \cdot b \cdot V \cdot P_0}{A \cdot R \cdot T_0} \quad (1)$$

where  $\text{Flux}_{\text{water-air}}$  (mg C m<sup>-2</sup> d<sup>-1</sup>) is the flux from the water surface to the atmosphere,  $M$  is the molar mass,  $b$  (mg L<sup>-1</sup> s<sup>-1</sup>) is the slope of the linear regression between the

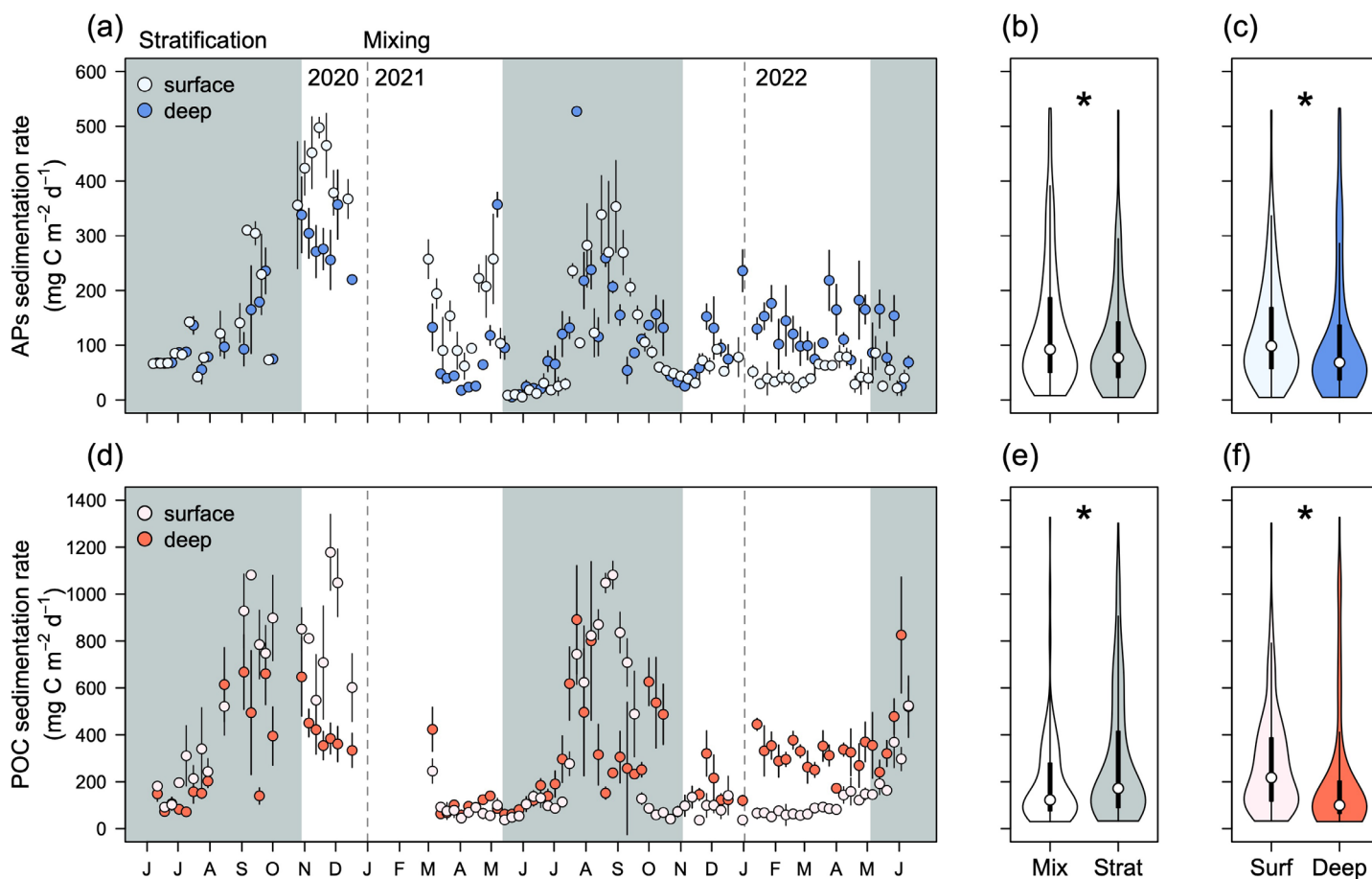


**Fig. 2.** Seasonal variation in sedimentation rates of APs and POC. Time series showing the variation in the sedimentation rate of APs (a) and POC (d) during the study period. The dots represent the mean values of the four sedimentation traps, while the lines display the 95% confidence interval (CI). The gray areas represent the stratification periods, whereas the white areas represent the mixing periods. The violin plots show the distribution of APs (b, c) and POC (e, f) sedimentation values when comparing mixing (Mix) and stratification (Strat) periods (b, e), and the surface and deep depths (d, f).



time (15–30 min) and the concentration of each gas inside the floating chamber,  $V$  (0.018 m<sup>3</sup>) and  $A$  (0.08 m<sup>2</sup>) are the volume and the area of the floating chamber,  $P_0$  (Pa) is the atmospheric pressure,  $R$  is the gas constant (8.314, m<sup>3</sup> Pa K<sup>-1</sup> mol<sup>-1</sup>), and  $T_0$  (K) is the atmospheric temperature. For the CH<sub>4</sub> fluxes, we discriminate between diffusion and ebullition using an adaptation of the algorithm proposed by Hoffmann et al. (2017). Briefly, the flux separation is dependent on identifying sudden changes in the slope  $b$  (flux rate) associated with ebullition during individual measurements. We

selected only the slopes significantly different from zero and with coefficients of determination ( $R^2$ ) higher than 0.85.

### Results and discussion

The APs sedimentation rates exhibited considerable variability spanning over two orders of magnitude from 4.54 to 532.90 mg C m<sup>-2</sup> d<sup>-1</sup>, showing a seasonal trend whereby the maximum sedimentation values occurred immediately after a stratification period in 2020, or during the stratification

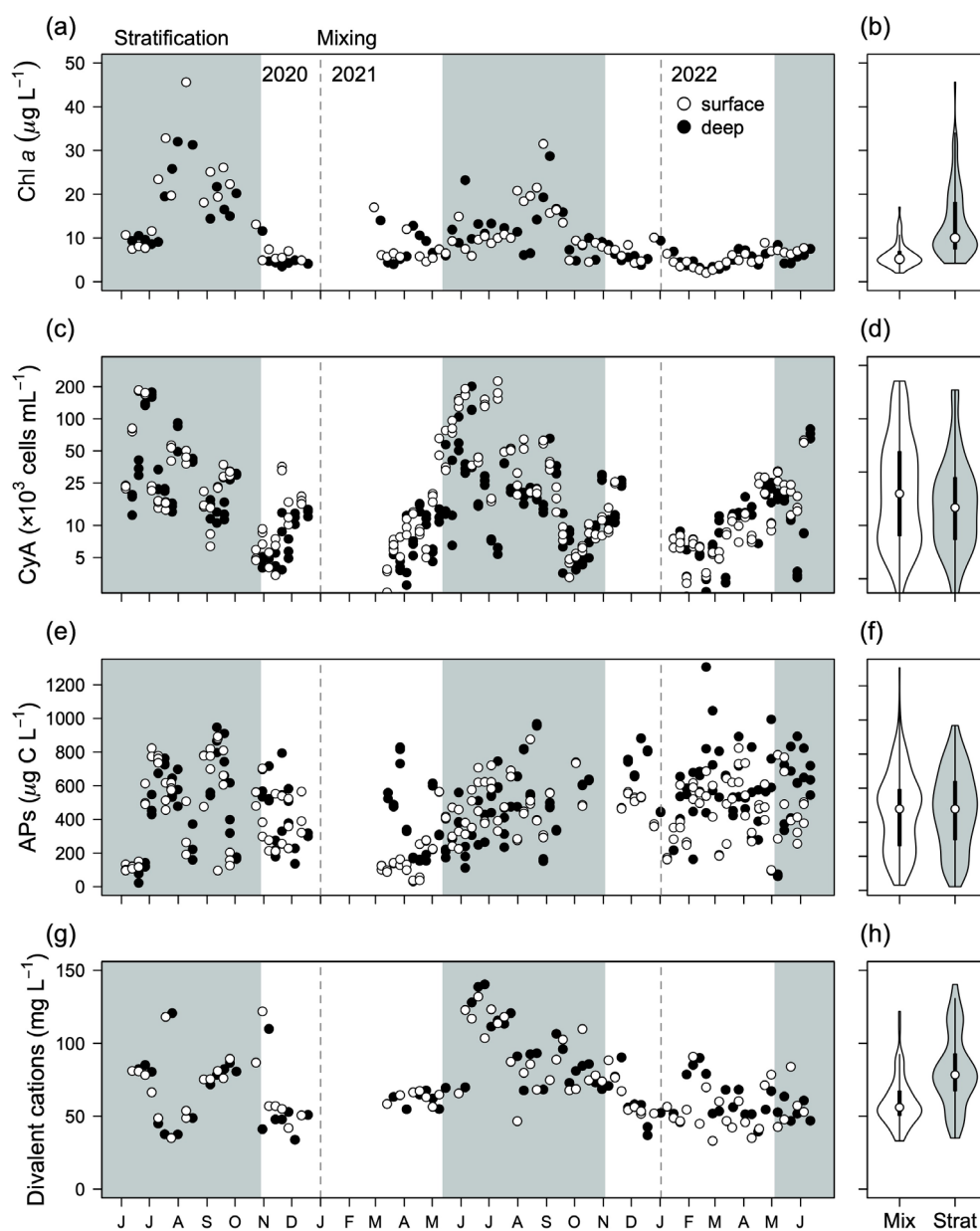


**Fig. 3.** Seasonal variations in the primary predictors influencing the sedimentation rates of APs and POC. The time series illustrates the changes in Chl *a* concentration (a), cyanobacterial abundance (CyA) (c), APs concentration (e), and concentration of divalent cations (f). The violin plots show the distribution of Chl *a* concentration (b), CyA (d), APs concentration (f), and divalent cations (Ca + Mg) (h) when comparing mixing (Mix) and stratification (Strat) periods.

in 2021 (Fig. 2a). Despite the minor differences between periods, the average APs sedimentation rates showed a higher trend during the mixing period and in the upper depth sections (Fig. 2b,c). On the other hand, the time series for POC sedimentation rates mirrored that of APs sedimentation rates (Fig. 2d), with a notably more pronounced tendency for POC sedimentation rates to be of greater magnitude during stratification periods (Fig. 2e). Moreover, the temporal variability of POC sedimentation rates was even more pronounced than that for APs, ranging from 30.29 to 1327.33 mg C m<sup>-2</sup> d<sup>-1</sup> (Fig. 2d). This is consistent with data previously reported for Mediterranean or boreal reservoirs (de Vicente et al. 2009; Teodoru et al. 2013). The great variability observed in POC sedimentation rates is nevertheless expected. While autochthonous sources predominantly contribute to APs, POC in reservoirs is shaped by the highly variable inputs from both autochthonous and allochthonous sources (von Wachenfeldt et al. 2008; de Vicente et al. 2009; Ye et al. 2023). Lastly, just as with APs sedimentation rates, we also noticed higher POC sedimentation rates at the surface layer than in the deep layer (Fig. 2f). This underscores the heightened biological activity in the surface and the key role of primary producers in organic matter export. It is worth mentioning here that our study does not account for the intricate trophic interactions between zooplankton and phytoplankton fractions. These interactions can influence the carbon flow in aquatic ecosystems (Yoshimizu et al. 2001; Kagami et al. 2006). In any case, the temporal variability observed in the sedimentation rates of APs and POC emphasizes the need to monitor processes that affect the carbon balance across various timescales.

The biological predictors examined also displayed great variability throughout the studied period. Chl *a* concentrations ranged from 2.0 to 45.6 μg L<sup>-1</sup> (Fig. 3a) with peak values toward the end of the summer, during stratification in

comparison with the mixing (Fig. 3b). Cyanobacterial abundance exhibited more than 100-fold variation between minimum and maximum values, ranging from 1.76 to 225.73 × 10<sup>3</sup> cells mL<sup>-1</sup> (Fig. 3c), with the highest abundances occurring in the surface during the stratification periods (Fig. 3d). APs concentration displayed a wide variation, ranging two orders of magnitude between the minimum and maximum values, from 22.09 to 1305.39 μg C L<sup>-1</sup> (Fig. 3e). The highest APs concentrations were observed between July and September in both depths, but without an apparent seasonal variability (Fig. 3f). The chemical predictors as the divalent cations (Ca + Mg), promoters of coagulation, ranged from 33.08 to 140.41 mg L<sup>-1</sup> (Fig. 3g), with higher values recorded during stratification periods (Fig. 3h).

The fitted models for both APs and POC sedimentation rates detected the differences between the sampling periods (mixing vs. stratification) and depth compartments (surface vs. deep). In the specific case of APs sedimentation rates, models also detected a positive effect of the Chl *a* and the cyanobacterial abundance, while a negative relationship with the divalent cations (Fig. 4a-c; see Supporting Information Table S2 for further details of model summary). These results are consistent with prior research suggesting that exopolymer particles primarily form and aggregate during the stationary, senescent, and autocatalytic phases of phytoplankton blooms, including cyanobacteria, in the photic, UV transparent waters (Passow 2002b; Berman-Frank et al. 2007; Ortega-Retuerta et al. 2009a; Callieri et al. 2017; Iuculano et al. 2017). Furthermore, our models support the widely accepted idea of that phytoplankton species are main producers of APs both in marine and freshwater ecosystems (Ortega-Retuerta et al. 2009b; de Vicente et al. 2010; Thornton 2014).

Considering our observed rise in Chl *a* and cyanobacterial abundance during summer stratification, our findings support the idea of that APs might increase under future warmer and longer stratification scenarios (Thornton 2014), potentially

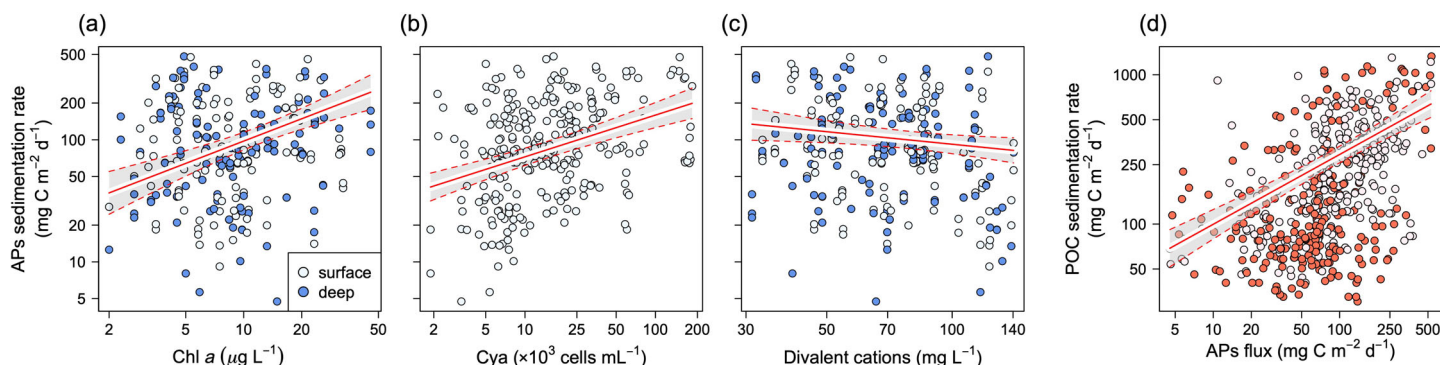


**Fig. 4.** Regression analysis showing the primary predictors of sedimentation rates for APs and POC. Factors driving the APs sedimentation rates encompass sampling period and depth (refer to Fig. 2), Chl *a* (a), surface cyanobacteria abundance (b), and divalent cations (c). For the POC sedimentation rates, predictors include sampling period and depth (refer to Fig. 2), and the sedimentation rates of APs (d). Dots depict the individual observations (262 for APs sedimentation rates and 336 for POC sedimentation rates), with solid lines representing the model's fit. The gray zones indicate the 95% confidence intervals around the predictions.

exacerbating APs fluxes toward sediments. On the contrary, the detected negative relationship between APs sedimentation rates and divalent cations seems to contrast with the fact that they promote ionic bridging between APs and enhance their

coagulation and subsequent sedimentation (Engel et al. 2004; Verdugo et al. 2004; Mari et al. 2017). De Vicente et al. (2010) also found this inverse trend between TEPs and divalent cations in Mediterranean inland waters, which is attributable to

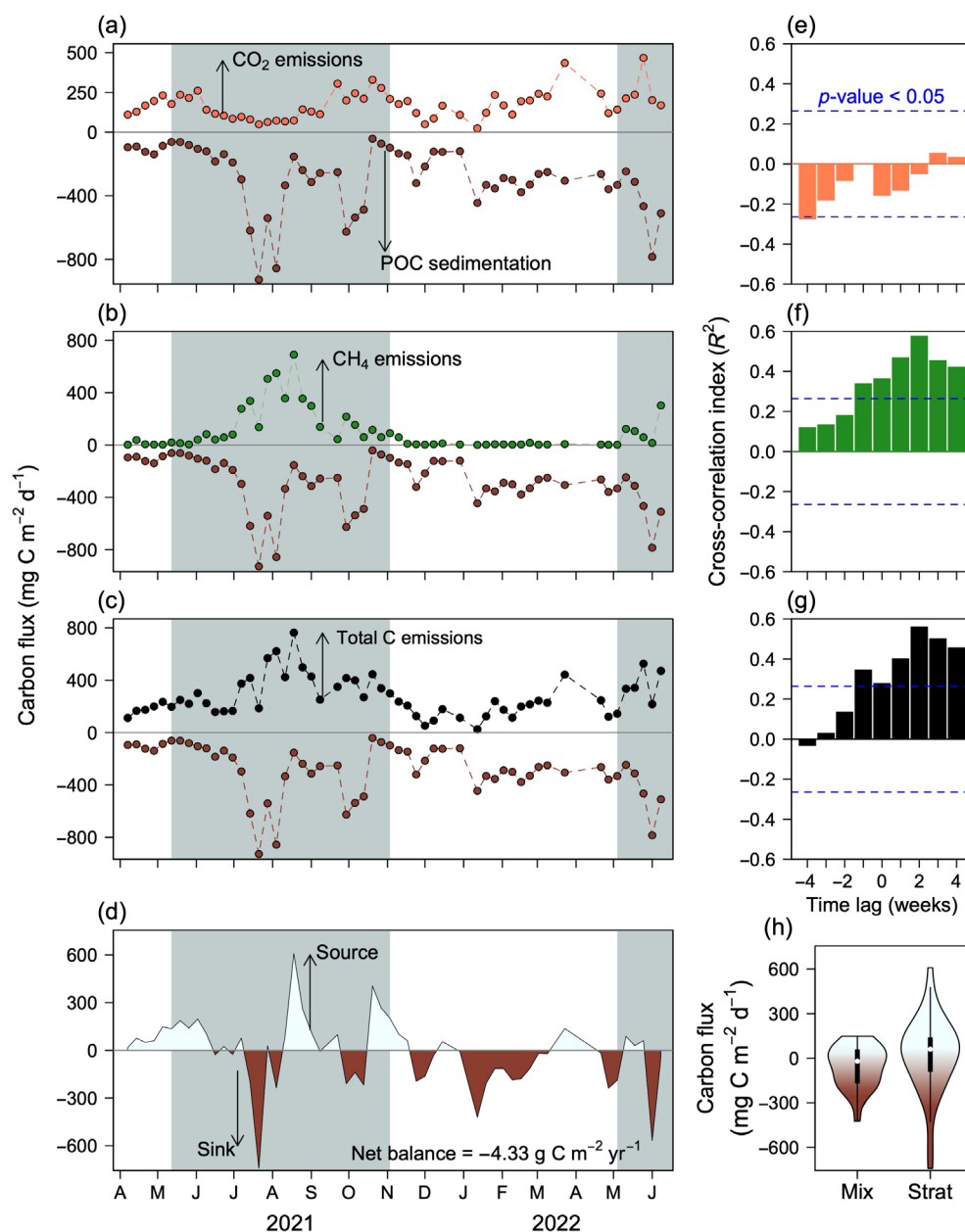


**Fig. 5.** Comparison of the carbon fluxes associated with the CO<sub>2</sub> and CH<sub>4</sub> seasonal emissions and carbon sedimentation rates in the study reservoir. Seasonal dynamics of POC sedimentation rate (negative values, brown dots) and CO<sub>2</sub> emissions (positive values, orange dots) including ebullitive and diffusive fluxes (positive values, green dots) (a), CH<sub>4</sub> emissions (positive values, green dots) (b), and the total carbon (CO<sub>2</sub> + CH<sub>4</sub>) emissions (positive values, black dots) (c). The carbon budgets between total emissions and POC sedimentation (d), represented as the light blue areas the moments when the reservoir acts as a net C source (emission > sedimentation, positive values) and the brown areas the periods the reservoir acts as a net C sink (sedimentation > emission, negative values). The figure also shows the cross-correlations between POC sedimentation rates and time series for CO<sub>2</sub> emissions (e) CH<sub>4</sub> emissions (f), and total carbon (CO<sub>2</sub> + CH<sub>4</sub>) emissions (g). The zero value in X-axis represents a synchronous dynamic without time-lags. The blue dashed lines represent the significant threshold ( $p < 0.05$ ). Bars above significant threshold represent time-lag correlation at weekly intervals. The violin plots show the distribution values of carbon net budgets when comparing between mixing (Mix) and stratification (Strat) periods.

a decrease in cation concentrations as they bind to the APs matrix, promoting sedimentation. This process of APs coagulation mediated by divalent cations still needs further exploration, particularly in inland waters with high ionic strength.

When examining the POC sedimentation rate, our models also identified the APs sedimentation rate itself as a strong predictor (Fig. 4d). Considering the strong synchrony observed between the sedimentation rates of APs and POC (Fig. 2a,d) and the relation of APs sedimentation rate and POC sedimentation (Fig. 4d, Supporting Information Table S3), we suggest that APs might influence the carbon sedimentation dynamics in the study reservoir. This result highlights that autochthonous polysaccharide production might play a key role in the carbon budget of freshwater ecosystems, and just as in marine ecosystems, it should be considered an essential pathway within the global carbon cycle. It should be mentioned that our approach remains descriptive, and despite the strong indications obtained in the field, future controlled experiments will be necessary to corroborate the proposed mechanisms underlying the POC sedimentation processes due to APs aggregation and sedimentation.

Lastly, we compare the carbon exported to sediments in the study reservoir (negative values) with the CO<sub>2</sub> (Fig. 5a), CH<sub>4</sub> (Fig. 5b), and total (CO<sub>2</sub> + CH<sub>4</sub>) (Fig. 5c) emissions (positive values) measured simultaneously by Rodríguez-Velasco et al. (unpublished data). The budget of these opposite fluxes (POC sedimentation vs. total emissions) in Fig. 5d represents the role of the study reservoir as a net source of carbon (positive values, light blue areas) or, on the contrary, as a net sink of carbon (negative values, brown areas) at contemporaneous time. Over the study period, we noted an alternating pattern where the reservoir sometimes acted as a net source (emissions > sedimentation) and at other times as a net sink (sedimentation > emissions) (Fig. 5d). By integrating and comparing the different emission and sedimentation periods and standardizing them over a year, we quantified an annual carbon budget with a total annual sinking rate of  $-4.33 \text{ g C m}^{-2} \text{ yr}^{-1}$ .

Previous studies at a spatial scale (Quadra et al. 2020) have reported a relationship between the burial rate of organic carbon and the CH<sub>4</sub> saturation in sediments (i.e., the potentiality for CH<sub>4</sub> emissions). Relatedly, Bertolet et al. (2020) found a correlation between the CH<sub>4</sub> storage within the hypolimnion and the mean summer rate of gross primary productivity across temperate lakes. However, we did not find synchronous correlations (i.e., time lag 0) between POC sedimentation rates and CO<sub>2</sub> (Fig. 5e), CH<sub>4</sub> (Fig. 5f), and total (Fig. 5g) emissions. Recent works (Isidorova et al. 2019b; Grasset et al. 2021) have experimentally demonstrated that the conversion of organic carbon into CH<sub>4</sub> takes from days to years, depending on organic matter quality (e.g., age, N content, and phytoplanktonic origin). In fact, we observed maximum cross-correlation index of the POC sedimentation on CH<sub>4</sub> emissions with a time lag of 2 weeks (Fig. 5f). Recently, Vizza et al. (2022) reported the existence of a 4-week time lag between CH<sub>4</sub>

production in sediments and CH<sub>4</sub> ebullition in temperate ponds at high latitudes in North America. These results indicate that POC might not be readily available as a substrate for the prokaryotic communities. Indeed, POC may need these 2 weeks period for assimilation by the prokaryotic community of the sediments and posterior CH<sub>4</sub> production and ebullition. However, the reservoir's role as an emitter exhibits a pronounced phenological pattern, with total gas emissions being considerably higher during stratification periods than during mixing periods ( $df = 23.465$ ,  $t = -2.364$ ,  $p = 0.03$ ; Fig. 5h). In contrast, the reservoir's role as a sink remained relatively similar when comparing between periods ( $df = 15.31$ ,  $t = 1.145$ ,  $p = 0.3$ ; Fig. 5h).

Although our quantification of the system's efficiency as a sink must be approached cautiously, to our knowledge, no such comprehensive and time-integrated budget for the Mediterranean biome as this one has been previously reported. This budget is especially relevant considering that Mediterranean latitudes contain the highest relative number of reservoirs globally, as Lehner and Döll (2004) noted. When taken as a whole, our research suggests that more comprehensive, time-integrated data are essential to ascertain the net role of reservoirs in the carbon cycle. This is particularly true when considering climate change projections anticipated to disrupt the natural phenology of reservoirs with an extension of the stratification period and potential deoxygenation of reservoirs (Jane et al. 2021; Woolway et al. 2021, 2022) and a concomitant increase of eutrophication (Beaulieu et al. 2019). Therefore, relying only on sporadic data can overshadow the inherent temporal fluctuations and overlook the delayed interplay between these carbon sinking and emission processes in reservoirs.

## References

- American Public Health Association (APHA), American Waterworks Association, and Water Environment Federation. 1992. *Standard methods for the examination of water and wastewater*, 18th ed. American Public Health Association.
- Anderson, N. J., H. Bennion, and F. Lotter. 2014. Lake eutrophication and its implications for organic carbon sequestration in Europe. *Glob. Change Biol.* **20**: 2741–2751. doi:10.1111/gcb.12584
- Anderson, N. J., A. J. Heathcote, and D. R. Engstrom. 2020. Anthropogenic alteration of nutrient supply increases the global freshwater carbon sink. *Sci. Adv.* **6**: 21–45. doi:10.1126/sciadv.aaw2145
- Attermeyer, K., S. Andersson, N. Catalán, K. Einarsdottir, M. Groeneveld, A. J. Székely, and L. J. Tranvik. 2019. Potential terrestrial influence on transparent exopolymer particle concentrations in boreal freshwaters. *Limnol. Oceanogr.* **64**: 2455–2466. doi:10.1002/lno.11197
- Barros, N., J. J. Cole, L. J. Tranvik, Y. Prairie, D. Bastviken, V. L. M. Huszar, P. A. Del Giorgio, and F. Roland. 2011. Carbon emission from hydroelectric reservoirs linked to



- reservoir age and latitude. *Nat. Geosci.* **4**: 593–596. doi:[10.1038/ngeo1211](https://doi.org/10.1038/ngeo1211)
- Battin, T. J., S. Luyssaert, L. A. Kaplan, A. K. Aufdenkampe, A. Richter, and L. J. Tranvik. 2009. The boundless carbon cycle. *Nat. Geosci.* **2**: 598–600. doi:[10.1038/ngeo618](https://doi.org/10.1038/ngeo618)
- Beaulieu, J. J., T. DelSontro, and J. A. Downing. 2019. Eutrophication will increase methane emissions from lakes and impoundments during the 21st century. *Nat. Commun.* **10**: 1375. doi:[10.1038/s41467-019-09100-5](https://doi.org/10.1038/s41467-019-09100-5)
- Berman-Frank, I., G. Rosenberg, O. Levitan, L. Haramaty, and X. Mari. 2007. Coupling between autocatalytic cell death and transparent exopolymeric particle production in the marine cyanobacterium *Trichodesmium*. *Environ. Microbiol.* **9**: 1415–1422. doi:[10.1111/j.1462-2920.2007.01257](https://doi.org/10.1111/j.1462-2920.2007.01257)
- Bertolet, B. L., C. R. Olson, D. K. Szydlowski, C. T. Solomon, and S. E. Jones. 2020. Methane and primary productivity in lakes: Divergence of temporal and spatial relationships. *J. Geophys. Res. Biogeosci.* **125**: e2020JG005864. doi:[10.1029/2020JG005864](https://doi.org/10.1029/2020JG005864)
- Callieri, C., G. Corno, M. Contesini, D. Fontaneto, and R. Bertoni. 2017. Transparent exopolymer particles (TEP) are driven by chlorophyll a and mainly confined to the euphotic zone in a deep subalpine lake. *Inland waters* **7**: 118–127. doi:[10.1080/20442041.2017.1294384](https://doi.org/10.1080/20442041.2017.1294384)
- Carlson, R. E. 1977. A trophic state index for lakes. *Limnol. Oceanogr.* **22**: 361–369. doi:[10.4319/lo.1977.22.2.0361](https://doi.org/10.4319/lo.1977.22.2.0361)
- Cartapanis, O., E. D. Galbraith, D. Bianchi, and S. L. Jaccard. 2018. Carbon burial in deep-sea sediment and implications for oceanic inventories of carbon and alkalinity over the last glacial cycle. *Clim. Past* **14**: 1819–1850. doi:[10.5194/cp-14-1819-2018](https://doi.org/10.5194/cp-14-1819-2018)
- Cole, J. J., and others. 2007. Plumbing the global carbon cycle: Integrating inland waters into the terrestrial carbon budget. *Ecosystems* **10**: 171–184. doi:[10.1007/s10021-006-9013-8](https://doi.org/10.1007/s10021-006-9013-8)
- Danger, M., B. Allard, M. B. Arnous, J. F. Carrias, J. Mériguet, L. Ten-Hage, and G. Lacroix. 2012. Effects of food-web structure on the quantity and the elemental quality of sedimenting material in shallow lakes. *Hydrobiologia* **679**: 251–266. doi:[10.1007/s10750-011-0890-2](https://doi.org/10.1007/s10750-011-0890-2)
- de Vicente, I., E. Ortega-Retuerta, O. Romera, R. Morales-Baquero, and I. Reche. 2009. Contribution of transparent exopolymer particles to carbon sinking flux in an oligotrophic reservoir. *Biogeochemistry* **9**: 13–23. doi:[10.1007/s10533-009-9342-8](https://doi.org/10.1007/s10533-009-9342-8)
- de Vicente, I., E. Ortega-Retuerta, I. P. Mazuecos, M. L. Pace, J. J. Cole, and I. Reche. 2010. Variation in transparent exopolymer particles in relation to biological and chemical factors in two contrasting lake districts. *Aquat. Sci.* **72**: 443–453. doi:[10.1007/s00027-010-0147-6](https://doi.org/10.1007/s00027-010-0147-6)
- Deemer, B. R., and others. 2016. Greenhouse gas emissions from reservoir water surfaces: A new global synthesis. *Bioscience* **66**: 949–964. doi:[10.1093/biosci/biw117](https://doi.org/10.1093/biosci/biw117)
- Engel, A. 2000. The role of transparent exopolymer particles (TEP) in the increase in apparent particle stickiness ( $\alpha$ ) during the decline of a diatom bloom. *J. Plankton Res.* **22**: 485–497. doi:[10.1093/plankt/22.3.485](https://doi.org/10.1093/plankt/22.3.485)
- Engel, A., S. Thoms, U. Riebesell, E. Rochelle-Newall, and I. Zondervan. 2004. Polysaccharide aggregation as a potential sink of marine dissolved organic carbon. *Nature* **428**: 929–932. doi:[10.1038/nature02453](https://doi.org/10.1038/nature02453)
- Gasol, J. M., and P. A. del Giorgio. 2000. Using flow cytometry for counting natural planktonic bacteria and understanding the structure of planktonic bacterial communities. *Sci. Mar.* **64**: 197–224. doi:[10.3989/scimar.2000.64n2197](https://doi.org/10.3989/scimar.2000.64n2197)
- Golub, M., and others. 2023. Diel, seasonal, and inter-annual variation in carbon dioxide effluxes from lakes and reservoirs. *Environ. Res. Lett.* **18**: 034046. doi:[10.1088/1748-9326/acb834](https://doi.org/10.1088/1748-9326/acb834)
- Grasset, C., S. Moras, A. Isidorova, R. M. Couture, A. Linkhorst, and S. Sobek. 2021. An empirical model to predict methane production in inland water sediment from particular organic matter supply and reactivity. *Limnol. Oceanogr.* **66**: 3643–3655. doi:[10.1002/lno.11905](https://doi.org/10.1002/lno.11905)
- Heiri, O., A. F. Lotter, and G. Lemcke. 2001. Loss on ignition as a method for estimating organic and carbonate content in sediments: Reproducibility and comparability of results. *J. Paleolimnol.* **25**: 101–110. doi:[10.1023/A:1008119611481](https://doi.org/10.1023/A:1008119611481)
- Hoffmann, M., M. Schulz-Hanke, J. G. Alba, N. Jurisch, U. Hagemann, T. Sachs, M. Sommer, and J. Augustin. 2017. A simple calculation algorithm to separate high-resolution CH<sub>4</sub> flux measurements into ebullition- and diffusion-derived components. *Atmos. Meas. Tech.* **10**: 109–118. doi:[10.5194/amt-10-109-2017](https://doi.org/10.5194/amt-10-109-2017)
- Huang, C., Z. Chen, Y. Gao, Y. Luo, T. Huang, A. Zhu, H. Yang, and B. Yang. 2019. Enhanced mineralization of sedimentary organic carbon induced by excess carbon from phytoplankton in a eutrophic plateau lake. *J. Soil. Sediment.* **19**: 2613–2623. doi:[10.1007/s11368-019-02261-2](https://doi.org/10.1007/s11368-019-02261-2)
- Isidorova, A., R. Mendonça, and S. Sobek. 2019a. Reduced mineralization of terrestrial OC in anoxic sediment suggests enhanced burial efficiency in reservoirs compared to other depositional environments. *Eur. J. Vasc. Endovasc. Surg.* **124**: 678–688. doi:[10.1029/2018JG004823](https://doi.org/10.1029/2018JG004823)
- Isidorova, A., C. Grasset, R. Mendonça, and S. Sobek. 2019b. Methane formation in tropical reservoirs predicted from sediment age and nitrogen. *Sci. Rep.* **9**: 1–9. doi:[10.1038/s41598-019-47346-7](https://doi.org/10.1038/s41598-019-47346-7)
- Iuculano, F., I. P. Mazuecos, I. Reche, and S. Agustí. 2017. Prochlorococcus as a possible source for transparent exopolymer particles (TEP). *Front. Microbiol.* **8**: 709. doi:[10.3389/fmicb.2017.00709](https://doi.org/10.3389/fmicb.2017.00709)
- Jane, S. F., and others. 2021. Widespread deoxygenation of temperate lakes. *Nature* **594**: 66–70. doi:[10.1038/s41586-021-03550-y](https://doi.org/10.1038/s41586-021-03550-y)
- Jansen, J., and others. 2022. Global increase in methane production under future warming of lake bottom waters. *Global Change Biol.* **28**: 5427–5440. doi:[10.1111/gcb.16298](https://doi.org/10.1111/gcb.16298)

- Kagami, M., T. B. Gurung, T. Yoshida, and J. Urabe. 2006. To sink or to be lysed? Contrasting fate of two large phytoplankton species in Lake Biwa. *Limnol. Oceanogr.* **51**: 2775–2786. doi:[10.4319/lo.2006.51.6.2775](https://doi.org/10.4319/lo.2006.51.6.2775)
- Kozerski, H. P. 1994. Possibilities and limitations of sediment traps to measure sedimentation and resuspension. *Hydrobiologia* **284**: 93–100. doi:[10.1007/BF00005734](https://doi.org/10.1007/BF00005734)
- Lehner, B., and P. Döll. 2004. Development and validation of a global database of lakes, reservoirs and wetlands. *J. Hydrol.* **296**: 1–4. doi:[10.1016/j.jhydrol.2004.03.028](https://doi.org/10.1016/j.jhydrol.2004.03.028)
- León-Palmero, E., R. Morales-Baquero, and I. Reche. 2020a. Greenhouse gas fluxes from reservoirs determined by watershed lithology, morphometry, and anthropogenic pressure. *Environ. Res. Lett.* **15**: 044012. doi:[10.1088/1748-9326/ab7467](https://doi.org/10.1088/1748-9326/ab7467)
- León-Palmero, E., A. Contreras-Ruiz, A. Sierra, R. Morales-Baquero, and I. Reche. 2020b. Dissolved CH<sub>4</sub> coupled to photosynthetic picoeukaryotes in oxic waters and to cumulative chlorophyll *a* in anoxic waters of reservoirs. *Biogeosciences* **17**: 3223–3245. doi:[10.5194/bg-17-3223-2020](https://doi.org/10.5194/bg-17-3223-2020)
- Liu, L., B. Qin, G. Zhu, Y. Zhang, G. Gao, Z. Gong, and Q. Huang. 2015. Distribution of dissolved acidic polysaccharides (dAPS) during cyanobacteria blooms in northern lake Taihu. *Limnology* **16**: 21–29. doi:[10.1007/s10201-014-0435-2](https://doi.org/10.1007/s10201-014-0435-2)
- Mari, X., U. Passow, C. Migon, A. B. Burd, and L. Legendre. 2017. Transparent exopolymer particles: Effects on carbon cycling in the ocean. *Prog. Oceanogr.* **151**: 13–37. doi:[10.1016/j.pocan.2016.11.002](https://doi.org/10.1016/j.pocan.2016.11.002)
- Mendonça, R., R. A. Müller, D. Clow, C. Verpoorter, P. Raymond, L. J. Tranvik, and S. Sobek. 2017. Organic carbon burial in global lakes and reservoirs. *Nat. Comm.* **8**: 16–94. doi:[10.1038/s41467-017-01789-6](https://doi.org/10.1038/s41467-017-01789-6)
- Morales-Pineda, M., B. Úbeda, A. Cózar, B. Obrador, and J. Á. Gálvez. 2016. Organic carbon sedimentation dominates over CO<sub>2</sub> emission in two net heterotrophic Mediterranean reservoirs during stratification. *Aquat. Sci.* **78**: 279–290. doi:[10.1007/s00027-015-0423-6](https://doi.org/10.1007/s00027-015-0423-6)
- Ortega-Retuerta, E., C. M. Duarte, and I. Reche. 2010. Significance of bacterial activity for the distribution and dynamics of transparent exopolymer particles in the Mediterranean Sea. *Microb. Ecol.* **59**: 808–818. doi:[10.1007/s00248-010-9640-7](https://doi.org/10.1007/s00248-010-9640-7)
- Ortega-Retuerta, E., U. Passow, C. M. Duarte, and I. Reche. 2009a. Effects of ultraviolet B radiation on (not so) transparent exopolymer particles. *Biogeosciences* **6**: 3071–3080. doi:[10.5194/bg-6-3071-2009](https://doi.org/10.5194/bg-6-3071-2009)
- Ortega-Retuerta, E., I. Reche, E. Pulido-Villena, S. Agustí, and C. M. Duarte. 2009b. Uncoupled distributions of transparent exopolymer particles (TEP) and dissolved carbohydrates in the Southern Ocean. *Mar. Chem.* **115**: 59–65. doi:[10.1016/j.marchem.2009.06.004](https://doi.org/10.1016/j.marchem.2009.06.004)
- Passow, U. 2002a. Transparent exopolymer particles (TEP) in aquatic environments. *Prog. Oceanogr.* **55**: 287–333. doi:[10.1016/S0079-6611\(02\)00138-6](https://doi.org/10.1016/S0079-6611(02)00138-6)
- Passow, U. 2002b. Production of transparent exopolymer particles (TEP) by phyto- and Bacterioplankton. *Mar. Ecol. Prog. Ser.* **236**: 1–12. doi:[10.3354/meps236001](https://doi.org/10.3354/meps236001)
- Quadra, G. R., S. Sobek, J. R. Paranaíba, A. Isidorova, F. Roland, R. do Vale, and R. Mendonça. 2020. High organic carbon burial but high potential for methane ebullition in the sediments of an Amazonian hydroelectric reservoir. *Biogeosciences* **17**: 1495–1505. doi:[10.5194/bg-17-1495-2020](https://doi.org/10.5194/bg-17-1495-2020)
- R Core Team (2023). *R: A language and environment for statistical computing*. R Foundation for Statistical Computing. Available from <https://www.R-project.org/>
- Raymond, P. A., and others. 2013. Global carbon dioxide emissions from inland waters. *Nature* **503**: 355–359. doi:[10.1038/nature12760](https://doi.org/10.1038/nature12760)
- Sobek, S., E. Durisch-Kaiser, R. Zurbrügg, N. Wongfun, M. Wessels, N. Pasche, and B. Wehrli. 2009. Organic carbon burial efficiency in lake sediments controlled by oxygen exposure time and sediment source. *Limnol. Oceanogr.* **54**: 2243–2254. doi:[10.4319/lo.2009.54.6.2243](https://doi.org/10.4319/lo.2009.54.6.2243)
- Teodoru, C. R., P. A. del Giorgio, Y. T. Prairie, and A. St-Pierre. 2013. Depositional fluxes and sources of particulate carbon and nitrogen in natural lakes and a young boreal reservoir in Northern Québec. *Biogeochemistry* **113**: 323–339. doi:[10.1007/s10533-012-9760-x](https://doi.org/10.1007/s10533-012-9760-x)
- Thornton, D. C. O. 2014. Dissolved organic matter (DOM) release by phytoplankton in the contemporary and future ocean. *Eur. J. Phycol.* **49**: 20–46. doi:[10.1080/09670262.2013.875596](https://doi.org/10.1080/09670262.2013.875596)
- Thornton, D. C. O., E. M. Fejes, S. F. DiMarco, and K. M. Clancy. 2007. Measurement of acid polysaccharides in marine and freshwater samples using alcian blue. *Limnol. Oceanogr. Methods* **5**: 73–87. doi:[10.4319/lom.2007.5.73](https://doi.org/10.4319/lom.2007.5.73)
- Tranvik, L. J., and others. 2009. Lakes and reservoirs as regulators of carbon cycling and climate. *Limnol. Oceanogr.* **54**: 2298–2314. doi:[10.4319/lo.2009.54.6\\_part\\_2.2298](https://doi.org/10.4319/lo.2009.54.6_part_2.2298)
- Tranvik, L. J., J. J. Cole, and Y. T. Prairie. 2018. The study of carbon in inland waters—From isolated ecosystems to players in the global carbon cycle. *Limnol. Oceanogr. Lett.* **3**: 41–48. doi:[10.1002/lo2.10068](https://doi.org/10.1002/lo2.10068)
- Verdugo, P., A. L. Alldredge, F. Azam, D. L. Kirchman, U. Passow, and P. H. Santschi. 2004. The oceanic gel phase: A bridge in the DOM-POM continuum. *Mar. Chem.* **92**: 67–85. doi:[10.1016/j.marchem.2004.06.017](https://doi.org/10.1016/j.marchem.2004.06.017)
- Vizza, C., S. E. Jones, J. A. Hart, W. E. West, and G. A. Lamberti. 2022. Pond methane dynamics, from microbial communities to ecosystem budget, during summer in Alaska. *Limnol. Oceanogr.* **67**: 450–467. doi:[10.1002/lno.12003](https://doi.org/10.1002/lno.12003)
- von Wachenfeldt, E., and L. J. Tranvik. 2008. Sedimentation in Boreal Lakes—The role of flocculation of allochthonous dissolved organic matter in the water column. *Ecosystems* **11**: 803–814. doi:[10.1007/s10021-008-9162-z](https://doi.org/10.1007/s10021-008-9162-z)

- von Wachenfeldt, E., S. Sobek, D. Bastviken, and L. J. Tranvik. 2008. Linking allochthonous dissolved organic matter and boreal lake sediment carbon sequestration: The role of light-mediated flocculation. *Limnol. Oceanogr.* **53**: 2416–2426. doi:[10.4319/lo.2008.53.6.2416](https://doi.org/10.4319/lo.2008.53.6.2416)
- Woolway, R. L., and others. 2021. Phenological shifts in lake stratification under climate change. *Nat. Commun.* **12**: 2318. doi:[10.1038/s41467-021-22657-4](https://doi.org/10.1038/s41467-021-22657-4)
- Woolway, R. L., S. Sharma, and J. P. Smol. 2022. Lakes in hot water: The impact of a changing climate on aquatic ecosystems. *Bioscience* **72**: 1050–1061. doi:[10.1093/biosci/biac052](https://doi.org/10.1093/biosci/biac052)
- Ye, H., C. Tang, Y. Cao, and E. Hou. 2023. Sources and fates of particulate organic matter in inland waters with complex land use patterns. *Sci. Total Environ.* **877**: 162568. doi:[10.1016/j.scitotenv.2023.162568](https://doi.org/10.1016/j.scitotenv.2023.162568)
- Yoshimizu, C., T. Yoshida, M. Nakanishi, and J. Urabe. 2001. Effects of zooplankton on the sinking flux of organic carbon in Lake Biwa. *Limnology* **2**: 37–43. doi:[10.1007/s102010170014](https://doi.org/10.1007/s102010170014)
- Zhao, Y., B. F. Wu, and Y. Zeng. 2013. Spatial and temporal patterns of greenhouse gas emissions from three gorges

reservoir of China. *Biogeosciences* **10**: 1219–1230. doi:[10.5194/bg-10-1219-2013](https://doi.org/10.5194/bg-10-1219-2013)

### Acknowledgments

The authors express their gratitude to the reviewers, including the editorial panel, for their notable contributions in enhancing the manuscript. This research was funded by the projects QUAL21-011 (Modeling Nature) of the Consejería de Universidad, Investigación e Innovación of the Junta de Andalucía, Spain; COCOMAS (MTM2017-91054-EXP), CRONOS (RTI2018-098849-B-I00) of Spanish Ministry of Science, Innovation, and Universities, B.RNM.558.UGR20 of FEDER/Junta de Andalucía and QUAL21-011 (Modeling Nature) Consejería de Universidad, Investigación e Innovación of the Junta de Andalucía to JC, IR, and FJR. AM-G and ER-V were supported by FPU Ph.D. fellowships (FPU20/05804 and FPU 19/02161, respectively) from the Ministry of Universities. IP-M and FP are PAIDI postdoctoral fellows funded by Junta de Andalucía.

*Submitted 24 October 2023*

*Revised 18 January 2024*

*Accepted 23 January 2024*